Supplementary material for: **Temperature-dependent diffusion of H_2SO_4 in air at atmospherically relevant conditions: laboratory measurements using laminar flow technique**

by David Brus, Lenka Škrabalová, Erik Herrmann, Tinja Olenius, Tereza Trávničková, Ulla Makkonen and Joonas Merikanto

Tests of proper flow tube operation

The independence of the wall loss rate coefficient on flow rate was tested at T=298 K at three RH 5, 14 and 40 %; see Fig S1.

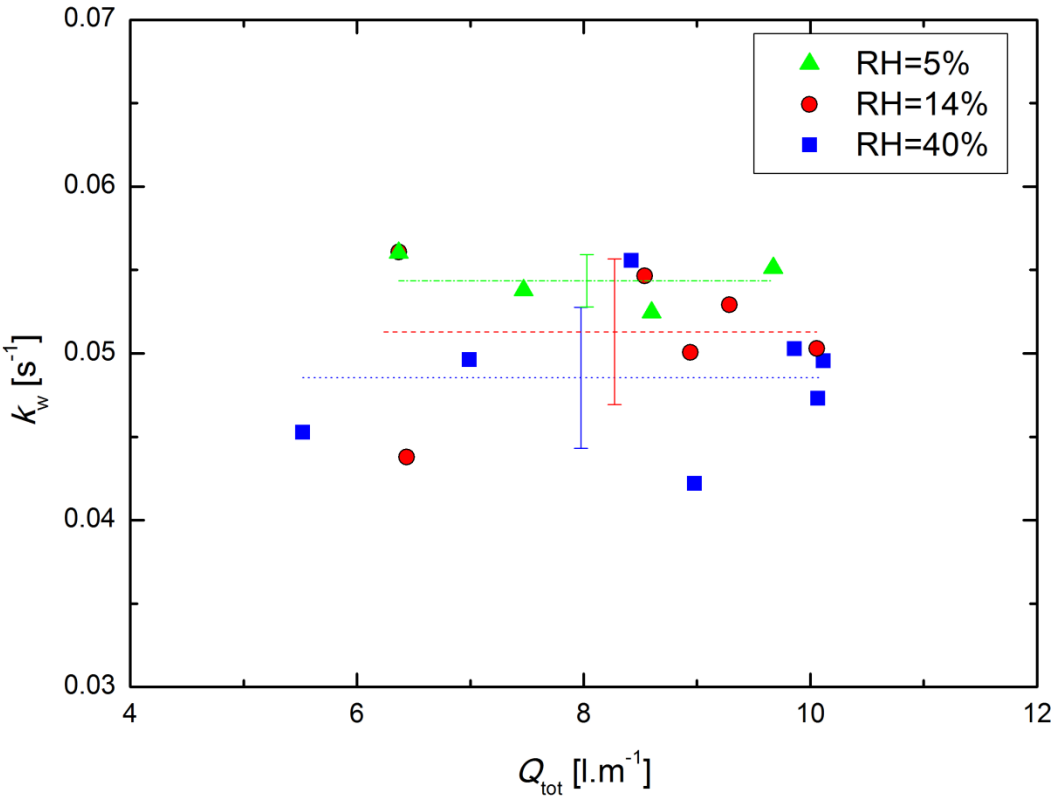

Fig S1. Measured wall loss rate coefficient as a function of total flow in the flow tube at three RHs 5, 14 and 40 %. Horizontal lines (separately for each RH) represent the mean, and the vertical error bars the standard deviation.

The independence on H_2SO_4 level, as well as data obtained when we *switched the flow tube parts* at *T*=298 K are covered in Fig S2. The tests were performed again at three RHs 5, 14 and 40 %.

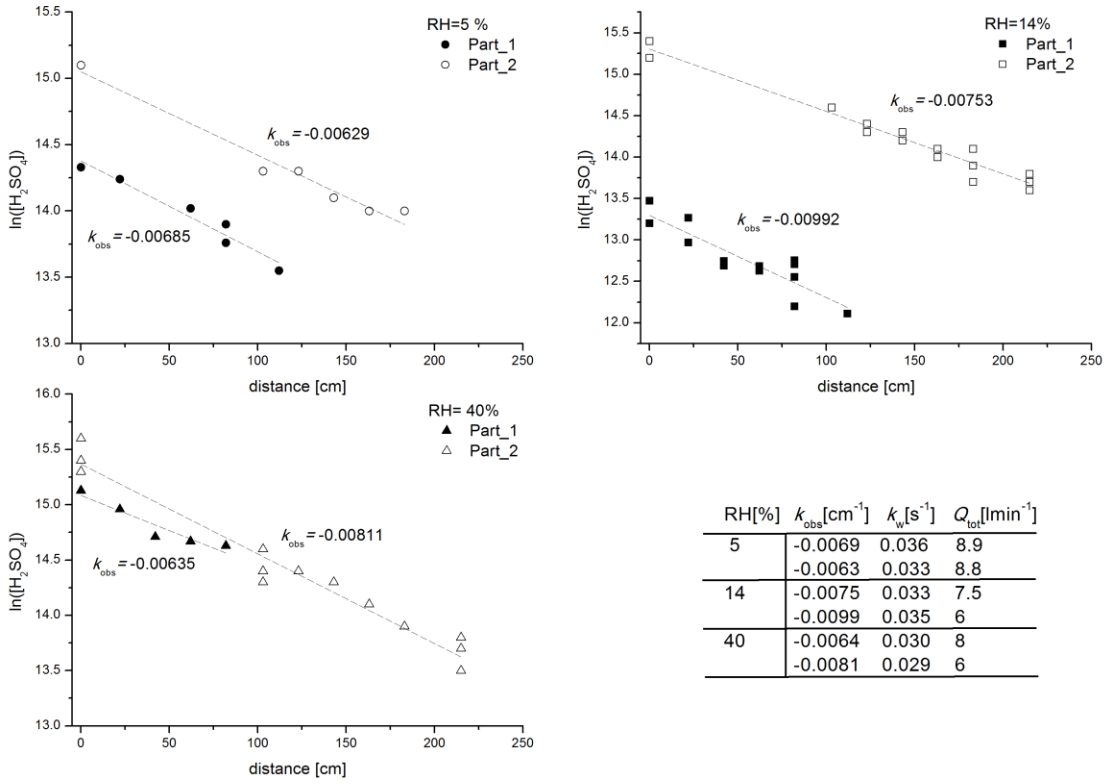

RH[%]	k_{obs}[cm^{-1}]	k_w[s^{-1}]	Q_{tot}[lmin^{-1}]
5	-0.0069	0.036	8.9
	-0.0063	0.033	8.8
14	-0.0075	0.033	7.5
	-0.0099	0.035	6
40	-0.0064	0.030	8
	-0.0081	0.029	6

Fig S2. Measured H_2SO_4 concentration as a function of distance in the flow tube at 298 K, at three RHs 5, 14 and 40 %, different levels of H_2SO_4 concentrations, and when the flow tube part with sampling ports is in the first half (0-100 cm, denoted as Part_1) or in the second half (100-200 cm, denoted as Part_2). The resulting wall loss rate coefficients k_w from the fits are presented in the table together with total flows Q_{tot} in the flow tube.

Measurements of impurities

Concentrations of impurities in our system were measured in two separate experiments. In the first experiment, saturator filled with neat sulfuric acid was used and measurements were conducted at dry conditions, each experiment at constant temperature took several hours. In the second experiment we tested if amines originate from the ultrapure water (Millipore, TOC less than 10 ppb, resistivity 18.2 MΩ.cm @25°C) used for humidification of the carrier gas. The same kind but another saturator was used as in experiment with sulfuric acid, see Fig 1 in manuscript.

MARGA (Monitor for Aerosols and Gas in Ambient Air system; Makkonen et al., 2012) with improved detection of amines by a quadrupole mass spectrometer (MS, Shimadzu LCMS-2020) was operated with electrospray ionization with positive mode. For quantitative analysis deuterated diethyl-

d10-amine (Sigma-Aldrich: Isotec™; Sigma-Aldrich, St. Louis, MO, USA) was used as an internal standard together with 3-point external calibration for all amines. Amines were detected as their M^{+1} ions and therefore impact of impurities with the same retention times but different molecular masses was removed. The limits of detection (LODs) were calculated as three times the standard deviation of the blank levels for di-methyl-amine (DMA) and tri-methyl-amine (TMA) and from signal-to-noise ratio (3:1) for mono-methyl-amine (MMA). LODs were 7 ppt for MMA, 1.7 ppt for DMA and 0.3 ppt for TMA.

Table ST1.The concentration of ammonia and amines in *ppt* measured in the first experiment at three temperatures (278, 288 and 298 K) in the saturator filled with sulfuric acid when purified air is used as carrier gas, all at dry conditions. MMA concentrations are provided even though they are below LOD, i.e. in practice zero.

	Ammonia	std(Ammonia)	MMA	std(MMA)	DMA	std(DMA)	TMA	std(TMA)
278 K	28.1	8.7	1.92	0.69	3.14	1.16	1.17	0.06
288 K	21.5	3.1	-	-	2.95	1.20	1.38	0.07
298 K	18.5	4.8	2.12	0.51	2.73	0.72	1.31	0.07

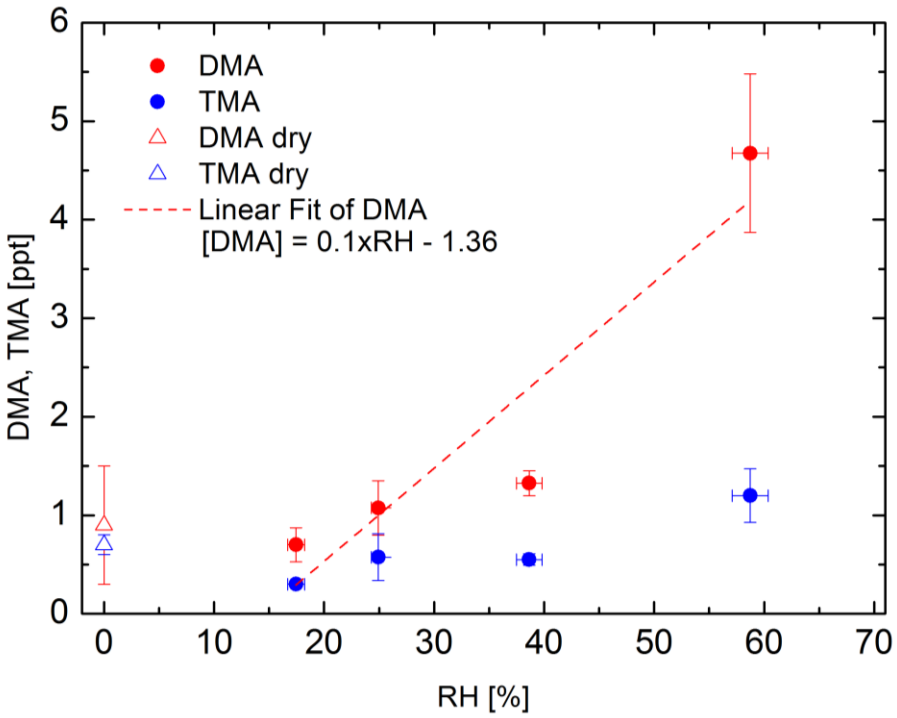

Fig S3. The concentration of amines in *ppt* measured by MS-MARGA in the second experiment as a function of RH, ultrapure water (Millipore, TOC less than 10 ppb, resistivity 18.2 MΩ.cm @25°C) was used to humidify the purified air. The amine RH dependency is flat up to about RH=18 %, TMA is almost flat compared to DMA, all MMA concentrations were found below LOD, thus not provided in figure. The linear fit to DMA data is valid only in the measured RH range 18-60 % with R^2=0.8.

Mathematical model

The model solves mass and momentum transport in the one phase system with H_2SO_4(g) and humid air as a carrier gas. During our simulations, we assume a 2D axisymmetric system, steady state, and incompressible fluid. Concentration of sulfuric acid and water vapor in carrier gas are supposed low without mutual interactions. The nonidealities connected to the mass transport of the H_2SO_4 molecules in the mixture are accounted in the value of the binary diffusion coefficient, which includes the presence of hydrates in the mixture. Also, thermal effects associated with mutual interactions between sulfuric acid and water molecules were neglected due to the overwhelming exceedance of the carrier gas that serves as thermostating agent. The modeling of transport processes uses Navier-Stokes equations to solve velocity profiles together with mass balance equation (Travnickova et al., 2013). Concentration profiles of sulfuric acid vapor are solved using convection–diffusion (scalar) equation. Particular components of the mixture enter the modelled part of flow tube at three different temperatures T=278, 288 and 298 K and atmospheric pressure p_{atm}. The model was solved in ANSYS Fluent 16.2 with following boundary conditions (see Table ST2):

Table ST2. Boundary conditions used for CFD simulations.

Inlet:	$z = 0$ $r \in \langle 0, R \rangle$	$v_z = \frac{2\dot{Q}}{\pi R^2}\left(1 - \left(\frac{r}{R}\right)^2\right)$ $v_r = 0$	$p = p_{atm}$ $[H_2SO_4] = [H_2SO_4]_{exp}\left(1 - \left(\frac{r}{R}\right)^2\right)$
Wall:	$z \in \langle 0, L \rangle$ $r = R$	$v_z = 0$ $v_r = 0$	$\frac{\partial p}{\partial r} = 0$ $[H_2SO_4] = 0$
Outlet:	$z = L$ $r \in \langle 0, R \rangle$	$\frac{\partial v_z}{\partial z} = 0$ $v_r = 0$	$p = p_{atm}$ $\frac{\partial [H_2SO_4]}{\partial z} = 0$
Symmetry:	$z \in \langle 0, L \rangle$ $r = 0$	$\frac{\partial v_z}{\partial r} = 0$ $v_r = 0$	$\frac{\partial p}{\partial r} = 0$ $\frac{\partial [H_2SO_4]}{\partial r} = 0$

where z and r are axial and radial coordinates respectively, R is radius of the flow tube, L is length of modelled part of flow tube, v_z, v_r are radial and axial velocities, p is pressure and $[H_2SO_4]$ is concentration of sulfuric acid. Subscript *exp* denotes experimental measured value.

Effects of grid discretisation

Our 2D uniform grid has a resolution 50 000 cells as it was used previously for the same experimental device in (Herrmann et al. 2010). Nevertheless, the dependence of $[H_2SO_4]$ on grid discretization was verified by refining of the grid from 50 000 to 200 000 cells. The deviation of maximal $[H_2SO_4]$ from the finest discretized case for all selected temperatures was less than one percent. For this reason, we suppose that our discretization with 50 000 cells is satisfactory and the results presented in this work

were computed on a mesh-independent grid. This method is commonly used and is described for example in (Travnickova et al., 2013).

Additional CFD simulations with different initial conditions and diffusion coefficients from the literature

To demonstrate the change in the losses inside the flow tube compared to our approach, we made the following set of CFD simulations for all three temperatures and a constant mid-range RH≈30%: a) we used the diffusion coefficient obtained from the experiment, but with a constant (flat-plug type) flow profile as initial condition, b) we used diffusion coefficients obtained from eq. (3) in Hanson and Eisele (2000) with the temperature dependency of $\sim T^{1.75}$ obtained from literature, and an initial parabolic flow profile. The simulations are summarized in Fig S4. Clearly, none of the two alternative approaches is able to reproduce the measured loss profile.

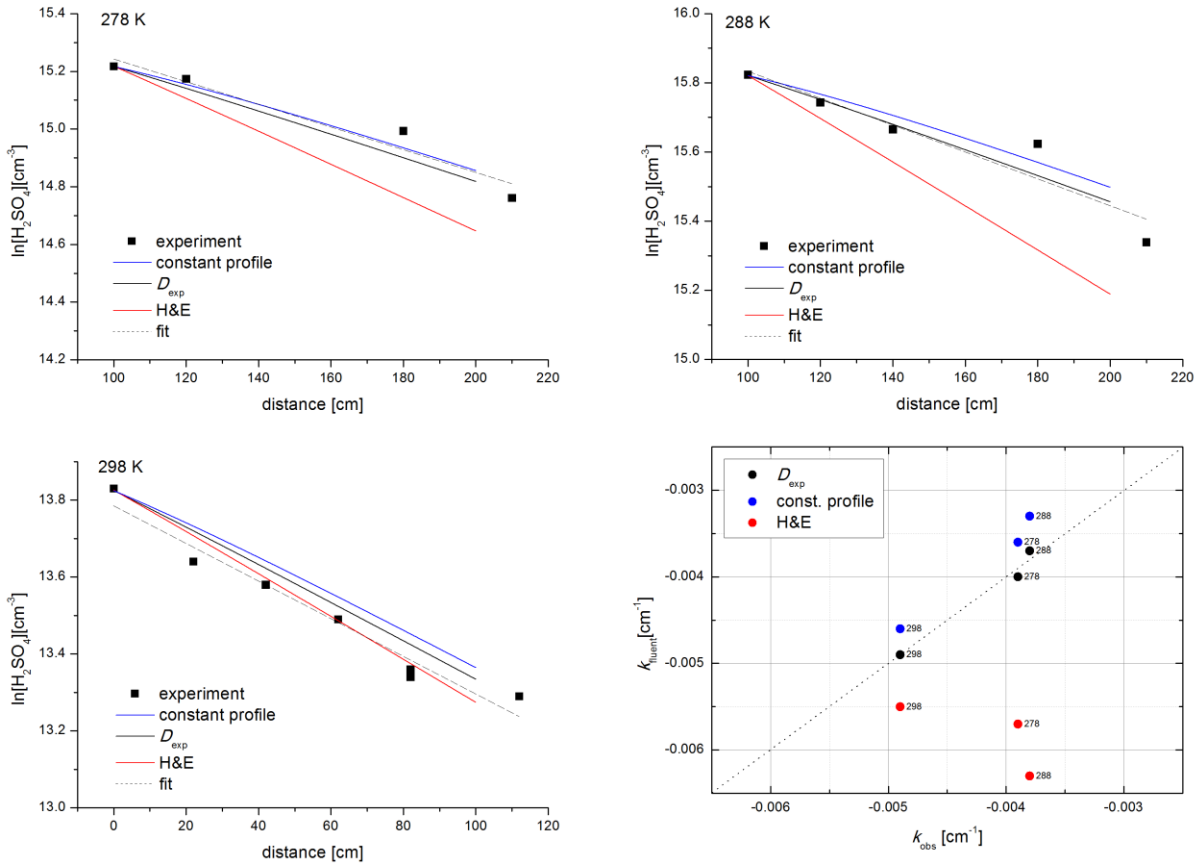

Fig S4. The sulfuric acid losses measured – black squares and simulated with CFD FLUENT model when the constant (flat-plug type) flow profile and the experimentally obtained diffusion coefficients are used as an initial condition - blue solid line; the diffusion coefficients obtained from eq. (3) in Hanson and Eisele (2000) and parabolic flow profile, red solid line; parabolic flow profile and the

experimentally obtained diffusion coefficients – black solid line and the fit to experimental data – black dashed line. All at T=278, 288 and 298 K. Simulated loss rate coefficients k_{fluent} (cm^{-1}) compared with experimental values of k_{obs} (cm^{-1}) at three different CFD setups and at T=278, 288 and 298 K, the dotted 1:1 line denotes the perfect agreement.

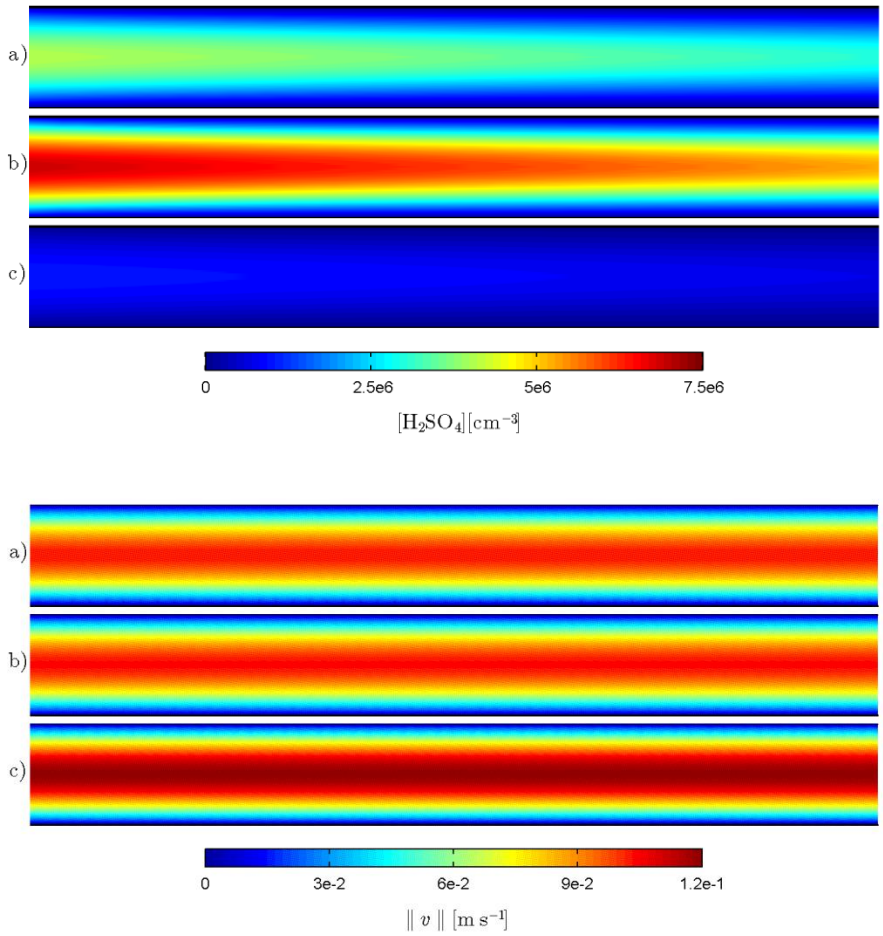

Fig S5. Example profiles of H_2SO_4 (top panel) and flow velocity (lower panel) for three temperatures T= a) 278, b) 288 and c) 298 K, the same CFD setup was used as above in Fig S4. Vertical axis is radius of the flow tube and horizontal axis is distance in the flow tube.

Details on quantum chemical data and cluster kinetics modelling

The simulations were run by setting initial concentrations for H_2SO_4 and base monomers, and integrating the time development of the cluster concentrations for the experimental residence times. The initial acid concentration was set to be the average H_2SO_4 monomer concentration $[H_2SO_4]= 5\times10^6$ cm^{-3} measured with CIMS at the beginning of the flow tube (in the manuscript see Fig. 1, hole 1) for all experimental conditions.

Theoretical diffusion coefficients for sulfuric acid and representative base contaminant molecules and small acid–base clusters and their hydrates were calculated according to the kinetic gas theory.

The simulations were performed for the three temperatures of 278, 288 and 298 K at atmospheric pressure (1 atm). The temperature dependence of the viscosity of the carrier gas, needed to calculate the diffusion coefficients of different species in the simulations (see Eq. (6) in Olenius et al., 2014), was taken to be:

$$\eta_{\mathrm{N}_2} = \eta_{\mathrm{N}_2,0} \left(\frac{T_0+C}{T+C}\right) \left(\frac{T}{T_0}\right)^{3/2},$$

where $\eta_{\mathrm{N}_2,0}$ = 17.81×10^{-6} Pa s, T_0 = 300.55 K, and C =111 K (Crane Co., 1982).

References

Hanson, D. R. and Eisele, F. L.: Diffusion of H_2SO_4 in humidified nitrogen Hydrated H_2SO_4, *J. Phys. Chem.* A, **2000**, 104, 1715–1719.

Makkonen, U., Virkkula, A., Mäntykenttä, J., Hakola, H., Keronen, P., Vakkari, V., and Aalto, P. P., Semi-continuous gas and inorganic aerosol measurements at a Finnish urban site: comparisons with filters, nitrogen in aerosol and gas phases, and aerosol acidity, *Atmos. Chem. Phys.*, **2012**, 12, 5617-5631, doi:10.5194/acp-12-5617-2012.

Herrmann, E., Brus, D., Hyvarinen, A.-P., Stratmann, F., Wilck, M., Lihavainen, H., and Kulmala, M., A Computational Fluid Dynamics Approach to Nucleation in the Water-Sulfuric Acid System, *J. Phys. Chem. A*, **2010**, *114*, 8033-42.

Travnickova, T., Havlica, J., and Zdimal, V., Description of fluid dynamics and coupled transports in models of a laminar flow diffusion chamber, *J. Chem. Phys.*, **2013**, 139, 14, doi: http://dx.doi.org/10.1063/1.4816963

Crane Co. and Crane Co. Engineering Division, 1982. Flow of Fluids Through Valves, Fittings, and Pipe, Crane Company, Technical paper.